J Radioanal Nucl Chem (2013) 298:639–650
DOI 10.1007/s10967-013-2471-5

Concentration of ^{238}U and ^{232}Th among constituent minerals of two igneous plutonic rocks exhibiting elevated natural radioactivity levels

A. Papadopoulos · G. Christofides · A. Koroneos · G. Poli

Received: 21 December 2012 / Published online: 26 March 2013

Abstract The concentrations of ^{238}U and ^{232}Th of the constituent minerals in two plutonic rock samples, from N. Greece, exhibiting elevated levels of bulk rock natural radioactivity were determined by using LA-ICP-MS. The available data of whole rock ^{238}U and ^{232}Th concentrations were also used. The minerals were separated using a combination of heavy liquids of various densities, shaking table and magnetic separation techniques. The great variation in the concentrations of ^{238}U and ^{232}Th is probably indicative of the different distribution of U and Th within the same rock, as well as to secondary post-magmatic processes that were responsible for the redistribution of U and Th. An estimation of the contribution of each mineral constituent to the natural radioactivity levels of the bulk rock is attempted. Thorite and zircon contribute the most to the whole rock ^{238}U and ^{232}Th content, while the contribution of apatite is moderate. The contribution of the rest of the minerals examined (fluorite, quartz, plagioclase, K-feldspar, amphibole, pyroxene, magnetite and biotite) is not important.

A. Papadopoulos (✉) · G. Christofides · A. Koroneos
Department of Mineralogy, Petrology and Economic Geology, School of Geology, Aristotle University of Thessaloniki, 541 24 Thessaloniki, Greece
e-mail: argpapad@geo.auth.gr

G. Christofides
e-mail: christof@geo.auth.gr

A. Koroneos
e-mail: koroneos@geo.auth.gr

G. Poli
Department of Earth Sciences, University of Perugia, Piazza Università, 06100 Perugia, Italy
e-mail: polig@unipg.it

Keywords Natural radioactivity · Uranium · Thorium · LA-ICP-MS · Granites · Radioactive minerals · Heavy liquid separation · Hydrothermal zircons

Introduction

Granitic rocks are composed of a variety of minerals. In spite of extensive existing data on the ^{238}U and ^{232}Th content of natural materials, previous works have focused almost entirely on bulk rocks and soils rather than individual constituent minerals.

In granitic rocks U and Th are mainly located in the crystal lattice of accessory and secondary minerals. However, they can be found as adsorbed ions in the grains of major minerals as well [1–5].

Elevated U and Th concentrations are usually exhibited by accessory minerals (e.g. zircon, apatite, sphene), which are present either as inclusions in major minerals, or as separate grains within the rock [2–4]. In some cases, allanite and epidote can be considered as major radioactive minerals [1, 2]. Monazite and xenotime are usually characterized by significant concentrations of radioactive elements, which are higher than those of zircon [1–4]. Uraninite and thorite, when found, contribute mostly to the total radioactivity of the rock [6]. Several less common minerals that in some cases are very radioactive, are uranothorite, thorianite, euxinite, pyrochloore, sevkinite, fluorite, davidite, hematite, pyrite, ilmenite and rutile [7].

The concentrations of ^{238}U and ^{232}Th of granitic rocks of Greece (124 studied samples) range from 0.11 to 21.59 ppm (mean 6.32 ± 4.1) and from 0.44 to 92.26 ppm (mean 20.96 ± 13.3) respectively [8]. Among them, sample MD2 (9.64 ppm U and 51.60 ppm Th), a medium grained granite of reddish color, from Fanos pluton and sample XMZ-501

(14.25 ppm U and 46.98 ppm Th), a medium grained bi-px quartz monzodiorite of grey color, from Xanthi pluton exhibited elevated levels of natural radioactivity. Both samples can be considered as representatives, in terms of U and Th concentrations, of the felsic and intermediate igneous plutonic rocks of Greece respectively. However, no sample of mafic composition was selected in this study, as none exhibits high U and Th concentrations.

In this study, ^{238}U and ^{232}Th concentrations of all the minerals present (major and accessory) in those two igneous plutonic samples were determined. Comparisons were made between the same minerals of the two samples. An attempt to correlate the modal mineralogical composition with the bulk rock radioactivity is also made. Finally considering U and Th geochemistry, the ^{232}Th/^{238}U ratios of the minerals analyzed are discussed.

Materials and methods

Geological setting

The plutonic bodies of Fanos and Xanthi are located in northern Greece (Fig. 1). The former intrudes the Vardar-Axios zone and the latter intrudes the Rhodope Massif.

Fanos pluton

The pluton intrudes the Vardar-Axios (Gevgeli) ophiolitic complex. It is composed of granite, microgranite and aplitic granite with granite being the prevailing rock-type [9]. The granite is mid-to coarse-grained and has a slightly reddish color. The aplitic granite occurs scarcely, mainly in the western region of the pluton. The major mineral constituents of the pluton are quartz, feldspar and biotite. Apatite, zircon, allanite and titanite are the accessory minerals of the pluton [10].

According to Christofides et al. [9], the pluton is peraluminous with calc-alkaline affinities. It has mainly I-type characteristics, but several S-type characteristics also occur [11, 12].

The pluton is associated with hydrothermal activity and molybdenite mineralization, principally along its western contact with the ophiolotic complex [13, 14].

According to Soldatos et al. [10], the Fanos pluton has derived by partial melting of infracrustal igneous rocks situated in the continental crust whereon the ophiolite has been obducted. However, sedimentary material may have contributed to the source, yet not changing considerably its compositional character.

Xanthi pluton

The Xanthi pluton is of Oligocene age [15–17], which intrudes mainly marbles, gneisses and Eocene sedimentary rocks of the upper tectonic unit of the Rhodope massif, as well as marbles belonging to the Lower Tectonic Unit. Mainly carbonates and skarn mineralization are present at contacts with metamorphic rocks. To the South, it is in tectonic contact with rocks of Neogene and Quaternary ages [16, 18].

The Xanthi pluton is distinguished into two main rock groups, the "acid" group and the "basic" group. The "acid" group, occupying the central and western part of the complex, comprises granodiorites grading into monzogranites bearing microgranular mafic enclaves of quartz diorite composition. The "basic" group occurs in the eastern part of the complex and is composed mainly of monzonite/quartz monzonite, quartz monzodiorite, and subordinate monzogabbro and olivine gabbro. The major mafic minerals of the pluton are quartz, feldspar, biotite, hornblende, pyroxenes (ortho- and clinopyroxenes), and olivine. Accessories are chlorite, sphene, apatite, zircon, rutile, epidote and opaque minerals (magnetite, ilmenite) [18].

The rock-types of the Xanthi pluton are calc-alkaline to high-K calc-alkaline with I-type characteristics [19, 20].

The most mafic rocks of the "basic" group and MME can be considered as mantle-derived magmas, and initial ratios of ^{87}Sr/^{86}Sr and ^{143}Nd/^{144}Nd claim for a K-enriched upper mantle source probably metasomatized by crustal components. The "acid" group magmas were generated through mantle-crust interaction. Trace element variations and Sr, Nd and Pb isotopic compositions indicate open-system evolutionary processes for the two groups, ruled by magma mixing rather than crustal assimilation [19, 20].

Sample preparation

Almost 30 kg for each sample was collected and crushed in order to separate adequate quantities of every constituent mineral. The grain size selected was 100–250 μm. Sample preparation and mineral separations were performed at the laboratories of the Department of Mineralogy, Petrology and Economic Geology, School of Geology, Aristotle University of Thessaloniki.

After washing and drying at room temperature, magnetite was separated using a hand magnet. Biotite was obtained by using a shaking table. The remainder of separated minerals (quartz, K-feldspar, plagioclase, zircon, apatite, amphibole, pyroxene, thorite and fluorite) was further separated, using heavy liquids (SPT, SPT carbide) of various densities and magnetic separator.

SEM–EDS-cathode luminescence

Among the grains of every mineral separated, several were carefully selected (hand-picking) for their euhedral shape, when possible, and lack of inclusions. One polished section

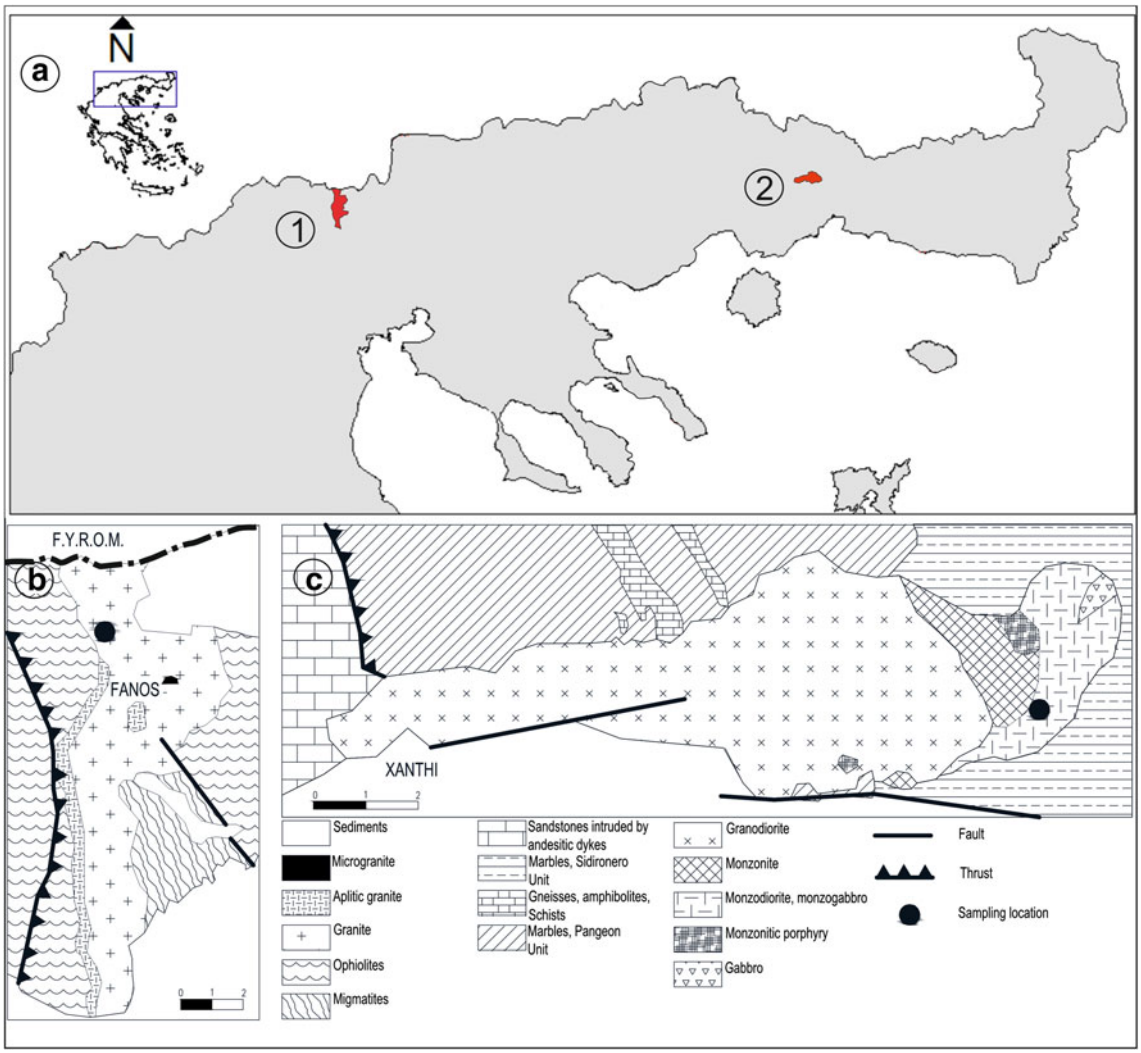

Fig. 1 **a** Sketch map of northern Greece with location of the plutons: *1*. Fanos pluton, *2*. Xanthi pluton. **b** Lithological map of Fanos pluton [9]. **c** Lithological map of Xanthi pluton [17]

was produced carrying the grains of both samples and was then studied under an EDS SEM at the Earth Science Department of the University of Siena. More specifically, both backscattered and cathode luminescence—CL (for determining zonations in zircons) images were taken, along with EDS analyses for mineral identification. SEM analyses were performed with a Philips XL30 device operated at 20 kV and equipped with an EDAX energy-dispersive (EDS) X-ray spectrometer.

LA-ICP-MS analysis

The LA-ICP-MS analyses were performed at the Department of Geosciences of the University of Perugia in Italy.

The ICP-MS system was a Thermo-Electron X7 (Thermo Electron Corporation, Waltham, USA), connected to a New Wave UP213 laser ablation unit. The later converts the laser ablation base frequency of 1064 to 213 nm by using three harmonic generators. In the sample holder of the machine can be installed simultaneously both the reference materials and the measured samples. Helium was used as a carrier gas in the sample holder, instead of argon, in order to enhance the carrying capacity. Then He was mixed with Ar before entering the ICP unit to ensure stable conditions stimulation. The repetition rate of the laser and its energy density were adjusted to 10 Hz and 10 J/cm^3 respectively.

Data processing was performed using the Glitter software. The detection limits for the U and Th, using a 40 microns laser diameter, is 0.002, and 0.002 mg/g.

More details on the instrumental set up and the analytical protocols for single-phase spatially-resolved and bulk trace-element analyses are presented by Petrelli et al. [21].

Results and discussion

The mineralogical composition of both samples which was determined by detailed point counting (>1800 points) is presented in Table 1.

The bulk rock ^{238}U and ^{232}Th specific activities (Bq/kg), the ^{238}U and ^{232}Th concentrations (ppm) and the values of ^{232}Th/^{238}U ratios (measured by gamma-ray spectroscopy) have been retrieved by Papadopoulos [8] and Papadopoulos et al. [22], are presented in Table 2.

The results of the LA-ICP-MS analysis are given in Tables 3 and 4 for the samples MD-2 and XMZ-501 respectively.

The range in the concentrations of ^{238}U and ^{232}Th in the same mineral is more or less high. Such range has been reported by previous researchers [1, 5, 7, 23–25]. What is more, the range is increasing with increasing concentrations of ^{238}U and ^{232}Th.

The average concentrations (ppm) of ^{238}U and ^{232}Th in the minerals of the sample MD-2 are <0.42 and 0.90 in plagioclase, <0.001 and <0.001 in quartz, 2.38 and 4.22 in biotite, 0.69 and 2.75 in magnetite, 0.185 and <0.001 in K-feldspar, 0.54 and 5.45 in fluorite, 2773 and 2811 in zircon, 49689 and 1167153 in thorite, and finally 21.99 and 177.9 in apatite.

The average concentrations (ppm) of the mineral constituents of the sample XMZ-501 in ^{238}U and ^{232}Th for quartz are <0.012 and <0.014 respectively, for K-feldspar is <0.07 and 4.97, for plagioclase 0.03 and 0.02, for biotite 0.43 and 0.27, for magnetite 0.60 and 0.41, the apatite 30.98 and 78.63, for pyroxenes 1.94 and 2.21, for amphiboles 0.60 and 0.64 ppm, and finally for zircon 674.4 and 592.

No reliable comparisons can be made among the concentrations of ^{238}U and ^{232}Th which are below 1 ppm (quartz, feldspars, biotite and magnetite), considering the ± standard errors. However (for the rest of the minerals) the minerals of the granitic sample (MD-2) have higher concentrations of ^{232}Th, than the more mafic one (XMZ-501). As for the ^{238}U, the same tendency is present, with the exception of apatite.

According to Table 2, the bulk rock concentrations of ^{238}U and ^{232}Th are 14 and 47 ppm respectively for the sample XMZ-501 and 9.6 ppm and 52 respectively for the sample MD-2. The ^{232}Th concentration of the granitic sample is higher than that of the monzodioritic one According to Faure [26], U- and Th-rich minerals are much more abundant in acid igneous rocks than in basic ones. This can be explained by the incompatibility of both U and Th during partial melting of the magma source and fractional crystallization processes (Kd < 1), leading thus in the remaining of U and Th in the melt and their incorporation in minerals of acid rocks. This is also confirmed by the fact that zircon rims are enriched in ^{238}U and ^{232}Th than zircon cores at all cases.

However, the ^{238}U concentration of sample MD-2 deviate the above mentioned rule, as the more mafic monzodioritic sample exhibits higher ^{238}U concentration than the granitic sample. This is likely to be indicative of U mobilisation over Th in the MD-2 sample and is reflected to the bulk rock ^{232}Th/^{238}U ratio (5.35), which is significantly different than the average granite value of 3.5 [27], while the bulk ^{232}Th/^{238}U ratio of XMZ-501 (3.30), is close to the average. A possible explanation to this could be the U mobilization and leaching due to the hydrothermal activity which is associated with the molybdenite mineralization in the Fanos area. According to Adams et al. [24] and Hoskin and Schaltegger [25], although U^{4+} is geochemically immobile, when it is oxidised to U^{6+}, or $(UO_2)^{2+}$ it becomes mobile and it can be leached and transported. On the other hand, Th is usually present as Th^{4+} which is geochemically immobile. Thus, the ^{232}Th/^{238}U ratio can be an indication of U mobilization.

Table 1 Modal mineralogical composition of the samples

	Qz	Kfs	Pl	Am	Bt	Px	Zrn	Ap	Op	Ep	Total
MD-2	36.8	30.6	28.1	0.0	3.1	0.0	0.5	0.3	0.6	0.0	100.0
XMZ-501	4.1	20.4	38.2	4.8	11.3	16.2	1.6	1.8	1.0	0.6	100.0

Qz quartz, *Kfs* K-feldspar, *Pl* plagioclase, *Am* amphibole, *Bt* biotite, *Px* pyroxene, *Zrn* zircon, *Ap* apatite, *Op* opaque minerals (magnetite), *Ep* epidote

Table 2 Specific activities (Bq/kg) and concentrations (ppm) of ^{238}U and ^{232}Th radioactive series [8, 22]

Sample	^{238}U radioactive series (Bq/kg)		^{232}Th radioactive series (Bq/kg)		^{238}U (ppm)	^{232}Th (ppm)	^{232}Th/^{238}U
	^{238}U	±σ	^{228}Ra	±σ			
MD-2	119.0	7.0	210.0	4.0	9.64	51.60	5.35
XMZ-501	175.8	6.6	191.2	4.7	14.25	46.98	3.30

Table 3 Concentrations of ^{238}U, ^{232}Th (ppm) and Th/U ratios in mineral grains from sample MD-2

		^{238}U	$\pm\sigma$	^{232}Th	$\pm\sigma$	Th/U
Quartz	Grain 1	bdl	–	bdl	–	–
	Grain 2	bdl	–	bdl	–	–
K-feldspar	Grain 1	0.185	0.043	bdl	–	–
	Grain 2	bdl	–	bdl	–	–
	Grain 3	bdl	–	bdl	–	–
	Grain 4	bdl	–	bdl	–	–
Plagioclase	grain 1	0.926	0.074	bdl	–	–
	Grain 2	0.244	0.053	0.139	0.033	0.57
	Grain 3	0.326	0.064	2.870	0.18	8.80
	Grain 4	0.128	0.046	0.219	0.044	1.71
	Grain 5	0.498	0.064	0.371	0.046	0.74
Biotite	Grain 1	2.16	0.23	7.24	0.5	3.35
	Grain 2	0.116	0.043	0.833	0.077	7.18
	Grain 3	bdl	–	0.96	0.12	–
	Grain 4	3.99	0.76	7.2	0.78	1.80
	Grain 5	3.77	0.22	4.29	0.26	1.14
	Grain 6	1.88	0.13	4.82	0.26	2.56
Magnetite	Grain 1	0.926	0.074	bdl	–	–
	Grain 2	0.18	0.17	0.062	0.059	0.34
	Grain 3	0.79	0.73	2.83	2.6	3.58
	Grain 4	1.27	1.19	5.19	4.82	4.09
Zircon	Grain 1 rim	4755.31	207.06	5942.48	307.87	1.25
	Grain 2 core	1070.58	46.73	1206.14	62.88	1.13
	Grain 3 core	1533.69	67.08	1309.18	68.24	0.85
	Grain 3 rim	5620.08	246.48	4646.74	243.08	0.83
	Grain 4 core	1450.38	63.78	818.75	43.01	0.56
	Grain 5 rim	4577.31	202.60	1745.55	92.51	0.38
	Grain 6 core	1329.73	59.12	2403.04	128.05	1.81
	Grain 7 rim	3801.06	169.75	1938.85	103.94	0.51
	Grain 8 core	2586.90	80.20	4390.64	186.24	1.70
	Grain 9 core	1005.95	38.09	3710.75	213.18	28.23
Apatite	Grain 1	34.37	1.13	98.84	3.99	2.88
	Grain 2	19.82	0.68	115.24	5.23	5.81
	Grain 3	21.67	0.74	469.67	7.74	7.83
	Grain 4	21.37	0.74	110.34	5.09	5.16
	Grain 5	15.49	0.54	107.99	5.02	6.97
	Grain 6	21.04	0.72	137.59	6.43	6.54
	Grain 7	29.32	1.00	248.62	11.69	8.48
	Grain 8	19.97	0.71	181.09	8.61	9.07
	Grain 9	21.91	0.75	174.83	8.36	7.98
	Grain 10	16.70	0.58	140.92	6.80	8.44
	Grain 11	20.22	0.71	171.39	8.34	8.48
Thorite	Grain 1	24076.91	54.89	1265128.63	69703.48	52.55
	Grain 2	20246.92	1098.45	884608.56	49117.62	43.69
	Grain 3	143509.66	929.35	1368827.38	76593.74	9.54
	Grain 4	81947.42	6625.89	1190088.00	67160.3	14.52
	Grain 5	91542.69	22543.77	2583980.75	45789.2	3.69
	Grain 6	22135.20	47.44	1000035.00	57989.96	45.18
	Grain 7	19420.73	1051.82	61976.50	57989.90	31.91
	Grain 8	24076.91	1450.48	1265128.63	3605.75	52.55
	Grain 9	20246.92	330.33	884608.56	4589.14	43.69

Table 3 continued

		^{238}U	$\pm\sigma$	^{232}Th	$\pm\sigma$	Th/U
Fluorite	Grain 1	0.312	0.044	14.85	0.72	47.60
	Grain 2	0.628	0.095	17.58	0.85	27.99
	Grain 3	0.113	0.03	bdl	–	–
	Grain 4	0.125	0.027	0.778	0.054	0.27
	Grain 5	1.545	0.09	bdl	–	–
	Grain 6	1.025	0.061	3.87	0.20	3.78
	Grain 7	0.681	0.06	1.002	0.078	1.47
	Grain 8	0.195	0.063	0.043	0.013	0.22
	Grain 9	0.266	0.031	0.037	0.031	0.14

What is more, the presence of oxidizing conditions (that could mobilize U) in the Fanos area can be proved by the reddish color of the granitic rock types of the pluton. Whitfield et al. [28] mention, that granites of reddish color contain an abnormally large amount of Th with low amounts of U, which is the case with sample MD-2.

Taking into account the contribution of each mineral constituent to the bulk rock concentrations of ^{238}U and ^{232}Th, it is clear that no mineral except zircon, thorite or apatite could control them, although such minerals account for less than 3.5 % of the mineralogical modal composition of the rock. Even in apatite, the concentrations of ^{238}U and ^{232}Th is a small fraction of those displayed by thorite or zircon. Th and U are stechiometric elements in the formula of thorite [(Th,U) SiO_4]. In the crystal lattice of zircon ($ZrSiO_4$), Zr can be substituted by U or Th as they have the same valence and their ionic radii are comparable to each other. Both U and Th can replace Ca in apatite [$Ca_{10}(PO_4)_6(OH,F,Cl,Br)_2$] but this can happen to a lot smaller extent due to differences in ionic radius and valence.

U and Th are not uniformly distributed within the rock forming minerals of the same pluton. This has also been reported by previous researchers e.g. [3, 4, 7, 23, 25, 29].

A different degree of alteration in the grains of the same mineral and the magmatic zoning in zircons are likely to be the reasons for this range. The presence of the large range of $^{232}Th/^{238}U$ ratios among the grains of the same mineral could be indicative of the different degree of alteration which was mentioned above.

As far as zircons are concerned, it is clear that zircon rims are enriched in ^{238}U and ^{232}Th than zircon cores. The distribution of U and Th in zircons has been discussed by previous researchers e.g. [30].

This is evident in sample XMZ-501 where $^{232}Th/^{238}U$ ranges from 1.03 to 3.90 and 0.71 to 1.05 in apatite and zircon respectively. On the other hand, the range of $^{232}Th/^{238}U$ ratios in apatite and zircon of the sample MD-2 are 2.88 to 9.07 and 0.38 to 52.55 respectively, revealing that Th and especially U has been redistributed.

As mentioned above, the $^{232}Th/^{238}U$ ratio of XMZ-501 sample is close to the typical average of granitic rocks, and thus no or small redistribution of U and Th has occurred. On the contrary, the MD-2 sample is affected by the hydrothermal solutions associated with the local molybdenite mineralization and/or oxidizing conditions during crystallization, thus U and Th have been redistributed within the mineral constituents of the pluton.

In Fig. 2(a–f), selected cathode luminescence and plain-polarized images of zircon grains from MD-2 and XMZ-501 samples are shown. Various evidence indicate the presence of hydrothermal zircons in sample MD-2. Figure 2c shows a zoned magmatic core mantled by a non-luminescent (black) rim, which is characteristic of hydrothermal zircons [31]; Fig. 2e illustrates the murky brown mantle and "spongy texture" due to a high frequency of fluid-inclusions in a zircon grain, being characteristic of hydrothermal origin [3, 31]. It is important to clarify that both of the previous textures are not presented by any zircon of the sample XMZ-501. Some of the zircon grains of the MD-2 sample exhibit elevated abundances of LREE (Data are available upon request), which is characteristic for hydrothermal zircons [31, 32]. The presence of hydrothermal zircons in the sample MD-2 and their absence in sample XMZ-501 can be concluded from the C1 chondrite-normalised [33] REE patterns of the zircons of both samples (Fig. 3). Generally, the HREE concentrations in zircons, is higher compared to that of LREE. This is due to the similar ionic radii of Zr^{4+} and HREE, in contrast to the larger ionic radii of LREE. The latter are generally incompatible in the zircon structure [25]. The chondrite-normalised patterns of magmatic zircons exhibit strong positive Ce anomaly, which is weak or absent in the hydrothermal zircons. Additionally, the hydrothermal zircons are generally enriched in REE than the magmatic ones. Hydrothermal zircons can be recognized in the discriminant diagrams (Sm/

Table 4 Concentrations of ^{238}U, ^{232}Th (ppm) and Th/U ratios in mineral grains from sample XMZ-501

		^{238}U	$\pm\sigma$	^{232}Th	$\pm\sigma$	Th/U
Quartz	Grain 1	bdl	–	bdl	–	–
	Grain 2	0.012	0.007	0.0143	0.0082	1.17
K-feldspar	Grain 1	0.0290	0.0012	0.009	0.007	0.30
	Grain 2	bdl	–	0.0230	0.0011	–
	Grain 3	bdl	–	0.0061	0.0005	–
	Grain 4	bdl	–	0.0109	0.0063	–
Plagioclase	Grain 1	bdl	–	–	–	–
	Grain 2	bdl	–	–	–	–
	Grain 3	bdl	–	0.033	0.009	–
	Grain 4	0.026	0.009	0.016	0.001	0.60
Biotite	grain 1	0.075	0.031	0.281	0.066	3.75
	Grain 2	0.79	0.11	0.256	0.067	0.32
Amphibole	Grain 1	1.394	0.082	1.189	0.088	0.85
	Grain 2	0.597	0.045	0.709	0.058	1.19
	Grain 3	0.336	0.03	0.501	0.045	1.49
	Grain 4	0.078	0.014	0.163	0.022	2.09
Pyroxene	Grain 1	1.509	0.079	4.38	0..22	2.90
	Grain 2	7.27	0.30	2.15	0.11	0.30
	Grain 3	0.285	0.039	0.65	0.02	2.29
	Grain 4	0.438	0.057	2.12	0.13	4.84
	Grain 5	0.289	0.049	0.573	0.048	1.98
	Grain 6	0.469	0.05	1.198	0.073	2.55
	Grain 7	0.422	0.049	0.971	0.063	2.30
	Grain 8	4.84	0.22	5.63	0.26	1.16
Magnetite	Grain 1	0.138	0.027	0.094	0.023	0.68
	Grain 2	0.573	0.081	1.42	0.19	2.48
	Grain 3	0.039	0.012	0.040	0.013	1.03
	Grain 4	1.90	0.25	0.11	0.03	0.06
	Grain 5	0.372	0.061	0.365	0.064	0.98

Table 4 continued

		^{238}U	$\pm\sigma$	^{232}Th	$\pm\sigma$	Th/U
Zircon	Grain 1 core	439.57	15.45	335.53	15.33	0.76
	Grain 2 core	204.32	7.20	145.02	6.68	0.71
	Grain 3 core	794.99	27.93	815.6	37.7	1.03
	Grain 4 core	561.61	19.82	431.77	20.15	0.77
	Grain 5 core	443.84	15.80	319.98	15.20	0.72
	Grain 6 core	620.73	22.17	555.06	26.58	0.89
	Grain 7 core	1048.50	37.59	910.09	43.96	0.87
	Grain 8 core	1054.99	37.95	693.12	33.77	0.66
	Grain 9 core	626.12	22.63	659.89	32.44	1.05
	Grain 10 core	396.00	14.4	358.73	17.81	0.91
	Grain 11 rim	1349.08	49.26	1236.46	61.91	0.92
	Grain 12 core	849.48	31.19	756.95	38.27	0.89
	Grain 13 core	735.86	27.14	747.07	38.10	1.02
	Grain 14 core	453.90	17.13	303.94	16.21	0.67
	Grain 15 core	479.92	18.17	500.39	26.81	1.04
	Grain 16 core	731.14	27.78	703.14	38.10	0.96
	Grain 17 core	879.70	28.98	561.21	18.89	0.64
	Grain 18 core	447.89	14.77	334.37	11.27	0.75
	Grain 19 core	835.61	27.59	561.75	18.96	0.67
	Grain 19 rim	1320.42	43.58	721.38	24.33	0.55
	Grain 20 rim	1235.46	40.82	1039.34	35.09	0.84
Apatite	Grain 1	31.29	1.15	68.32	3.37	2.18
	Grain 2	27.83	1.03	108.57	5.37	3.90
	Grain 3	42.55	1.55	43.8	2.20	1.03
	Grain 4	30.74	1.13	68.13	3.43	2.22
	Grain 5	30.60	1.15	94.49	4.79	3.09
	Grain 6	29.97	1.14	98.94	5.06	3.30
	Grain 7	30.46	1.15	73.31	3.78	2.41
	Grain 8	24.40	0.93	73.47	3.82	3.01

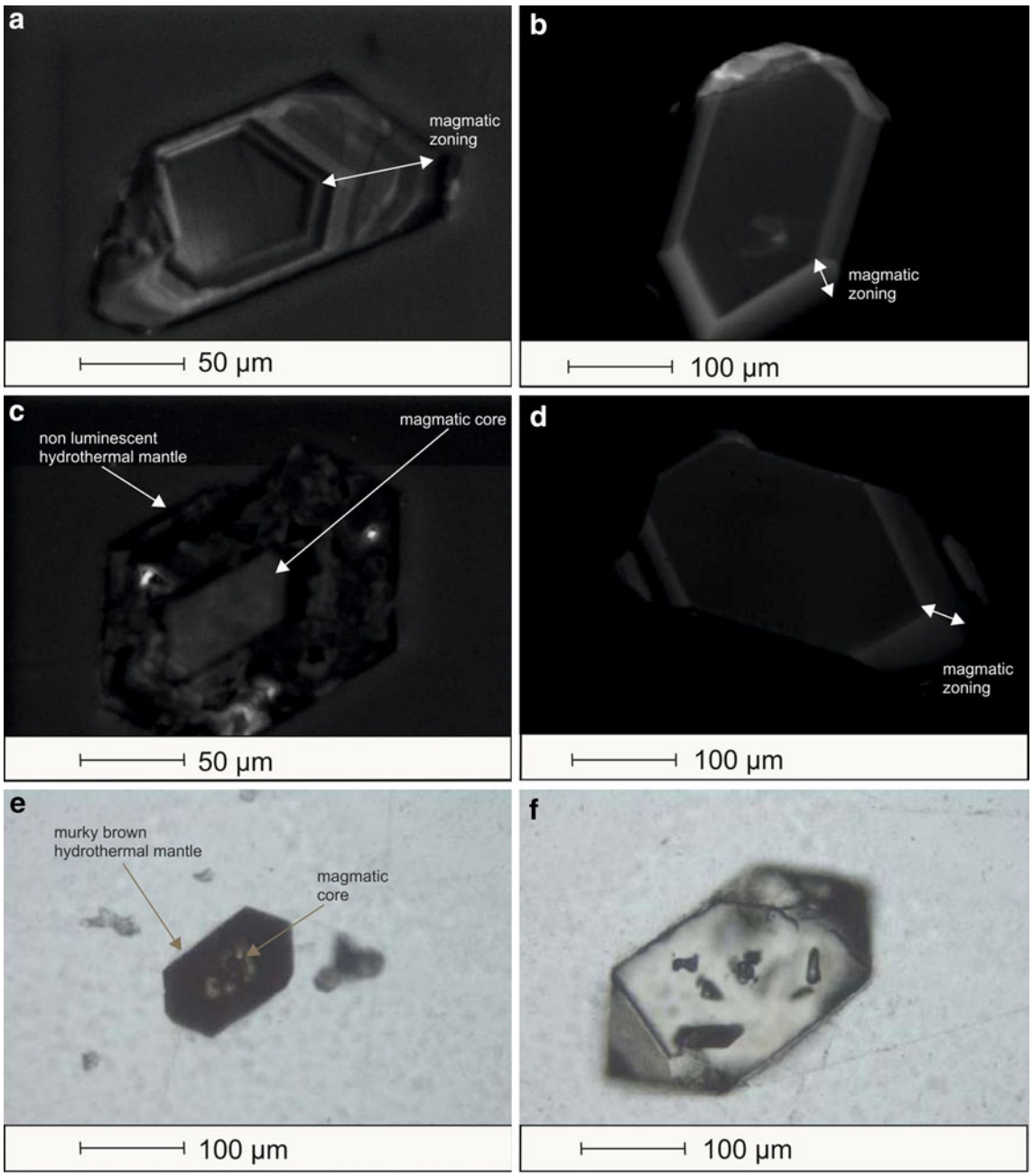

Fig. 2 Selected cathode luminescence and plain-polarized images of zircon grains from MD-2 and XMZ-501 samples. **a** CL image of MD-2 zircon, revealing typical magmatic zoning. **b** CL image of XMZ-501 zircon, revealing typical magmatic zoning. **c** CL image of MD-2 zircon, revealing a zoned magmatic core mantled by a non-luminescent (*black*) hydrothermal zircon mantle. **d** CL image of XMZ-501 zircon, revealing typical magmatic zoning. **e** Photomicrograph of a zircon crystal from MD-2 illustrating the *murky brown* hydrothermal mantle and 'spongy texture' due to a high frequency of fluid inclusions on an unaltered magmatic core (grain-mount, plain-polarized light). **f** Photomicrograph of a zircon crystal from XMZ-501. All the zircons of this sample are transparent (grain-mount, plain-polarized light)

La)N vs. La and Ce/Ce* vs. (Sm/La)N (Fig. 4a, b), proposed by Fu et al. [34].

Consequently, the presence of hydrothermal zircons in sample MD-2 could be a reason for the diversities in the distribution of both U and $^{232}Th/^{238}U$ values within the zircons and the bulk rock. On the other hand, their absence in sample XMZ-501 is likely to be the reason for the smaller range and diversity in U and Th distribution within the zircons and the bulk rock.

The variable distribution of U and Th in the zircons of sample MD-2 and controversially, the uniform distribution of U and Th in the zircons of sample XMZ-501 is presented in Fig. 5. However it is clear that even in the magmatic zircons of Fanos, U and Th are erratically distributed, probably due

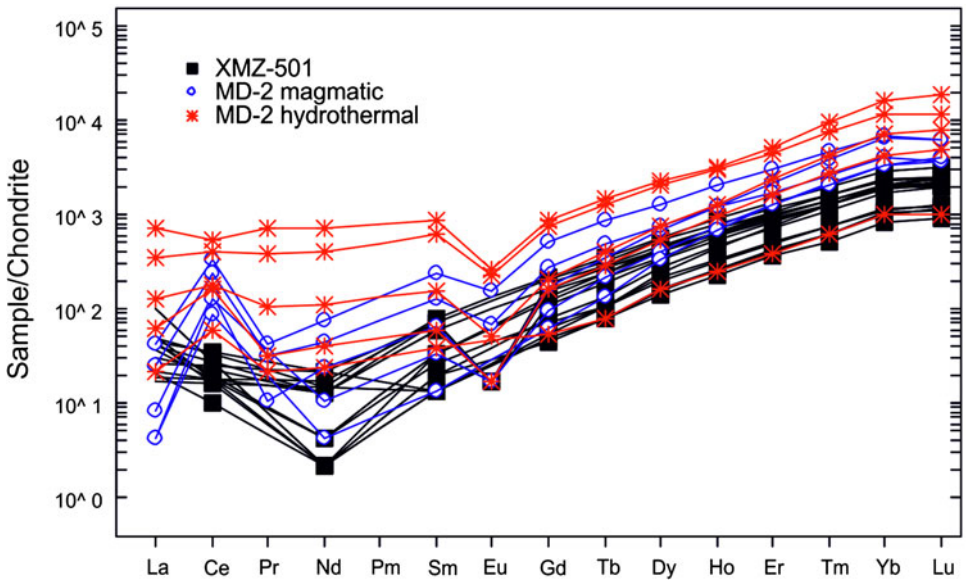

Fig. 3 Comparison of chondrite-normalized REE patterns for zircons from XMZ-501 and MD-2 samples

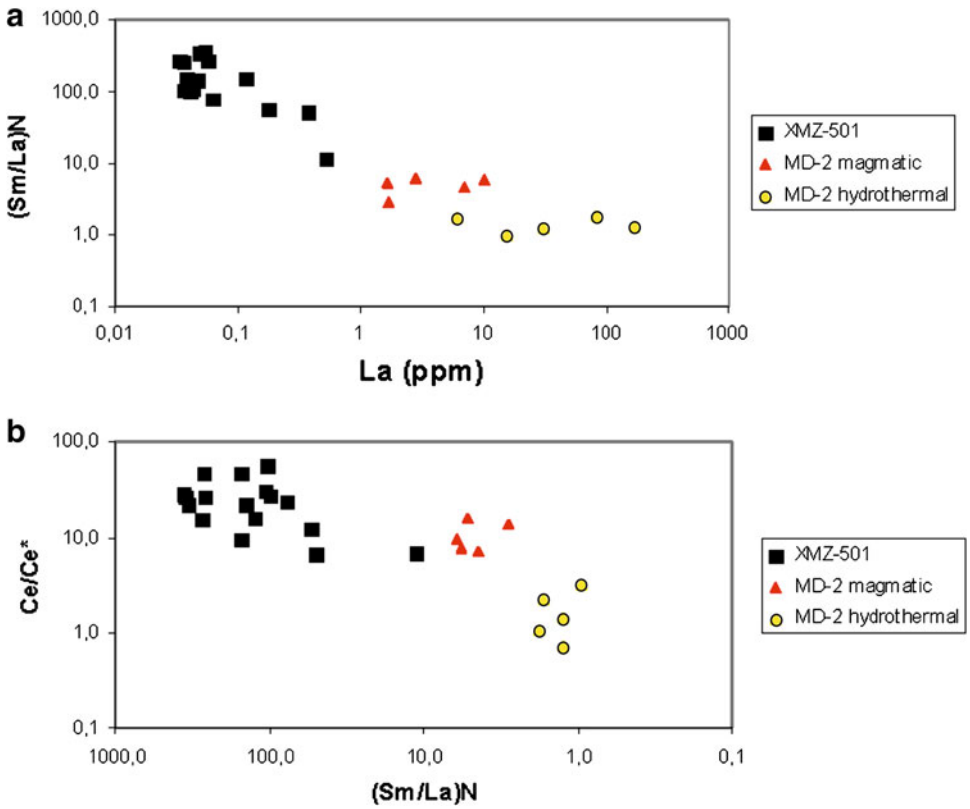

Fig. 4 Discriminant diagrams [34] of hydrothermal-magmatic zircons. **a** (Sm/La)N vs La (ppm). **b** Ce/Ce* vs (Sm/La)N for zircons of XMZ-501 and MD-2 samples. Ce/Ce* = (Ce/0.613)/SQRT ((La/0.237)*(Pr/0.0928)), (Sm/La)N = (Sm/0.148)/(La/0.237)

to the above mentioned oxidizing conditions, but in any case in less extent than the hydrothermal zircons.

Considering the $^{232}Th/^{238}U$ ratios in thorite and fluorite occurring in sample MD-2 (3.69–52.55 and 0.14–47.60 respectively) a rather huge range is present. This can be an indication that they are alteration products of the hydrothermal activity which is associated with the local molybdenite mineralization and not primary mineral occurrences. However, further investigation on the formation and origin of thorite and fluorite present in the Fanos pluton is necessary.

Finally, despite the detailed mineralogical analysis of both samples with point counting, no correlation is possible between any minerals and the bulk concentrations of U and Th. The large range in U and Th concentrations especially in zircon and thorite of the sample MD-2, is likely to be the reason for this.

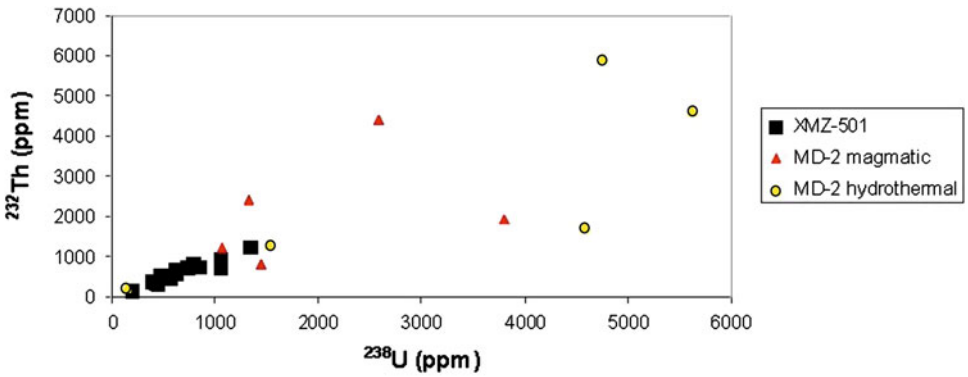

Fig. 5 ^{232}Th vs ^{238}U concentrations of the zircon grains of MD-2 and XMZ-501 samples

Conclusions

Generally, the minerals of the more felsic granitic sample from Fanos are more enriched in ^{238}U and ^{232}Th than those of the more mafic sample from Xanthi.

There is a very large range (variation) in the concentrations of ^{238}U and ^{232}Th among minerals of the same rock in all the minerals examined. This large variation observed, is probably due to the different distribution of U and Th in the rock, and magmatic and post-magmatic processes that could redistribute them.

Considering the ^{232}Th/^{238}U ratios of the minerals, there is also a lack of regularity between the grains of the same mineral in the same rock. However, the variation of the ^{232}Th/^{238}U ratio in the mineral constituents of the sample XMZ-501 is smaller than in sample MD-2, especially in apatite and zircon. This could be the result of (a) the intense hydrothermal activity which is associated with the local molybdenite mineralization, (b) the presence of oxidizing conditions (which are confirmed by the reddish color of the granite), and (c) the presence of both magmatic and hydrothermal zircons in sample MD-2.

The large range in the concentrations of both U and Th, especially in thorite and zircon which are the major U and Th carriers, makes unfeasible the correlation between bulk U and Th concentrations and the mineralogical composition of the rocks studied. Moreover, even in magmatic U and Th are not uniformly distributed between cores and rims.

Apatite can hardly be considered as a major U and Th carrier, as it contains only a fraction of the U and Th in zircon and thorite. Pyroxene, biotite, amphiboles, feldspars and quartz contain small or negligible amounts of U and Th.

References

1. De Voto RH (1978) Uranium in Phanerozoic sandstone and volcanic rocks. Short course in uranium deposits of the Gas Hills and Shirley Basin, Wyoming. Economic Geology 69:527–531
2. Deer WA, Howie RA, Zussman J (1992) An introduction to the Rock-Forming Minerals, 2nd edn. Longman, London, p 696
3. Hoskin PWO (2005) Trace-element composition of hydrothermal zircon and the alteration of Hadean zircon from the Jack Hills, Australia. Geochim Cosmochim Acta 69:637–648
4. Žáček V, Škoda R, Sulovský P (2009) U-Th-rich zircon, thorite and allanite-(Ce) as main carriers of radioactivity in the highly radioactive ultrapotassic melasyenite porphyry from the Šumava Mts., Moldanubian Zone, Czech Republic. J Geosci 54(4): 343–354
5. Sakoda A, Nishiyama Y, Hanamoto K, Ishimori Y, Yamamoto Y, Kataoka T, Kawabe A, Yamaoka K (2010) Differences of natural radioactivity and radon emanation fraction among constituent minerals of rock and soil. Appl Radiat Isot 68:1180–1184
6. Hamilton E (1958) Distribution of radioactivity in rocks and minerals and the effect of weathering on determination of uranium. Nature Lond. 181:697–698
7. Heinrich WME (1958) Mineralogy and geology of radioactive raw materials. McGraw-Hill Book Company, New York, 643p
8. Papadopoulos A (2011) Natural radioactivity in relation to mineralogy, geochemistry of uranium and thorium of magmatic rocks from Greece: Contribution to the use of natural building materials. Ph.D. Thesis, Aristotle University of Thessaloniki, p 283. (In Greek with English abstract)
9. Christofides G, Soldatos T, Koroneos A (1990) Geochemistry and evolution of the Fanos granite, N. Greece. Mineral Petrol 43:49–63
10. Soldatos T, Koroneos A, Christofides G (1993) Origin and evolution of the Fanos granite (Macedonia, Northern Greece): trace and REE modelling constraints. In Panagos's Honorary Volume. Technical University Publications B, Athens, pp 330–349
11. Christofides G, Koroneos A, Soldatos T, Eleftheriadis G (2000) Mesozoic magmatism in the area between the Vardar (Axios) zone and the Serbo-Macedonian massif (Northern Greece). In: Karamata S, Jankovic S (eds) Proceedings of the International Symposium on Geology and Metallogeny of the Dinarides and the Vardar Zone. Banja Luka 1:111–120
12. Saric K, Cvetkovic V, Romer RL, Christofides G, Koroneos A (2009) Granitoids associated with East Vardar ophiolites (Serbia, F.Y.R. of Macedonia and northern Greece): origin, evolution and geodynamic significance inferred from major and trace element data and Sr-Nd-Pb isotopes. Lithos 108: 131–150
13. Tsamantouridis P, Pergamalis F (1977) Report on the geological-economic geology mapping of the Fanos-Pigi area, Kilkis, IGME, Athens, 1–29, in Greek
14. Paraskevopoulos GM (1958) Die Bildungsverhaltnisse des molybdanlager Stadter des Gebiets von Axioupolis. Annales Géologiques des Pays Hélléniques I,9.260 pp

15. Liati A (1986) Regional metamorphism and overprinting contact metamorphism of the Rhodope zone, near Xanthi (N. Greece): Petrology, geochemistry, geochronology. Ph.D. Thesis, Techn. Univ. Braunschweig, p 186
16. Kyriakopoulos C (1987) Geochronological, geochemical, mineralogical and isotopic studies of the Tertiary plutonic rocks of the Rhodope. Ph.D thesis, Univ. of Athens, p 343 (In Greek with English abstract)
17. Christofides G, Pipera K, Koroneos A, Papadopoulos A (2012) New geochronological data from the Xanthi pluton: Constraints on the Nestos thrust dating. Proceedings of the International Congress "Geological Schools of Bulgaria, The School of prof. Zhivko Ivanov. "Exhumation of High-grade Metamorphic Rocks, Magmatic Arc Systems and Strike-slip Zones" Sofia, 2012
18. Christofides G (1977) Contribution to the study of plutonic rocks in the area of Xanthi. Ph.D. thesis, University of Thessaloniki, p 249 (in Greek with English abstract)
19. Christofides G, Soldatos T, Eleftheriadis G, Koroneos A (1998) Chemical and isotopic evidence for source contamination and crustal assimilation in the Hellenic Rhodope plutonic rocks. Acta Vulcanol 10(2):305–318
20. Bigazzi NSG, Christofides G, Del Moro A, Kyriakopoulos K (1994) A contribution to the evolution of the Xanthi pluton (Northern Greece): the apatite fission track analysis. Bollettino dellaSocietà Geologica Italiana 113:243–248
21. Petrelli M, Perugini D, Alagna KE, Poli G, Peccerillo A (2008) Spatially resolved and bulk trace element analysis by laser ablation—inductively coupled plasma –mass spectrometry (LA–ICP–MS). Periodico di Mineralogia 77:3
22. Papadopoulos A, Christofides G, Koroneos A, Stoulos S, Papatefanou C (2013) Radioactive secular equilibrium in ^{238}U and ^{232}Th series in granitoids from Greece. Appl Radiat Isotopes 75:95–104
23. Larsen ES, R J, Waring CL, Berman J (1953) Zoned zircon from Oklahoma. Amer. Mineral. 38:1118–1125
24. Adams JAS, Osmond YK, Rogers JJW (1959) The geochemistry of uranium and thorium. Phys Chem Earth 3:298–343
25. Hoskin PWO, Schaltegger U (2003) The composition of zircon and igneous and metamorphic petrogenesis. In: Hanchar J, Hoskin PWO, Mineralogical Society of America and Geochemical Society Reviews in Mineralogy and Geochemistry (eds) Zircon, 53rd edn., pp 27–62
26. Faure G (1986) Principles of Isotope Geology, 2nd edn. Wiley, London, p 464
27. Kyser K, Cuney M (2008) Recent and not -so recent developments in uranium deposits and implications for exploration. Mineral Assoc Can Short Course 39:257
28. Whitfield JM, Rogers JJW, Adams JAS (1959) The relationship between the petrology and the thorium and uranium contents of some granitic rocks. Geochim Cosmochim Acta 17:248–271
29. Pagel M (1982) The mineralogy and geochemistry of uranium, thorium and rare earth elements in two radioactive granites of the Vosges, France. Mineral Mag 46:151–163
30. Poller U, Huth J, Hoppe P, Williams IS (2001) REE, U, Th, and Hf distribution in zircon from Western Carpathian Variscan granitoids: a combined cathodoluminescence and ion microprobe study. Am J Sci 301:858–876
31. Hoskin PWO, Kinny PD, Wyborn D (1998) Chemistry of hydrothermal zircon: investigating timing and nature of water-rock interaction. In: Arehart GB, Hulston JR (eds) Water-Rock Interaction, WRI-9. AA Balkema, Rotterdam, pp 545–548
32. Rubin JN, Henry CD, Price JG (1989) Hydrothermal zircons and zircon overgrowths, Sierra Blanca Peaks, Texas. Am Mineral 74:865–869
33. McDonough WF, Sun S–S (1995) The composition of the Earth. Chem Geol 120:223–253
34. Fu B, Mernagh TP, Kita NT, Kemp AIS, Valley JW (2009) Distinguishing magmatic zircon from hydrothermal zircon: a case study from the Gidginbung high-sulphidation Au-Ag-(Cu) deposit, SE Australia. Chem Geol 259(3–4):131–142